Fermi gases in the two-dimensional to quasi-two-dimensional crossover

Chingyun Cheng,[1,2] J. Kangara,[1] I. Arakelyan,[1] and J. E. Thomas[1,*]

[1]*Department of Physics, North Carolina State University, Raleigh, North Carolina 27695, USA*

[2]*Department of Physics, Duke University, Durham, North Carolina 27708, USA*

We smoothly tune the dimensionality of pancake-shaped ^{6}Li Fermi gas clouds from quasi-two-dimensional to two-dimensional (2D) to measure radio-frequency spectra and cloud profiles in both regimes. In the quasi-2D case, where $E_F/h\nu_z \simeq 1$, with E_F the Fermi energy and $h\nu_z$ the harmonic oscillator energy in the tightly confined direction, we confirm that the radio-frequency spectra strongly disagree with 2D mean-field theory. Then we tune to the 2D regime, $E_F << h\nu_z$, where the measured radio-frequency spectra are in very good agreement with 2D mean-field theory. Nevertheless, the measured cloud profiles strongly disagree, confirming predictions that a beyond mean-field approach is required throughout the 2D to quasi-2D crossover.

Quasi-two-dimensional (quasi-2D) geometries play important roles in high-temperature superconductors [1], layered organic superconductors [2], and semiconductor interfaces [3]. In high-transition temperature copper oxide and organic superconductors, electrons are confined in a quasi-two-dimensional configuration, creating complex, strongly interacting many-body systems, for which the phase diagrams are not well understood [4]. Enhancement of the critical temperature T_c for the quasi-2D regime, as compared to the true 2D regime, has been predicted for thin films in parallel magnetic fields [5] and for quasi-2D Fermi gases containing atoms in excited states of the tightly confined direction [6], where T_c may exceed the 3D value. Ultracold atomic Fermi gases in 2D and quasi-2D geometries provide model systems, which have been the subject of numerous predictions [6–19] and experiments [20–32].

In 2D systems, the dimer binding energy $E_b \geqslant 0$ sets the natural scale of length for scattering interactions [33], but a many-body treatment is required for $E_F > E_b$, as the inter-atom spacing is then smaller than the dimer size. Two-dimensional-BCS mean-field theory (MFT) [7] provides an elegant treatment of this problem, but MFT is expected to fail in 2D systems, as noted by Randeria and Taylor [34] and shown by many recent predictions [15,16,18,35–38]. For quasi-2D systems, the effect of the third dimension on the equation of state and pairing energies is not yet understood [6,19].

Radio-frequency spectra obtained with $E_F/h\nu_z << 1$, in the nearly 2D regime [24,25], reveal that the absorption threshold is close to E_b, a 2D-BCS mean-field prediction [7] that one would not have expected to be quantitatively valid in 2D [34]. Although one might expect similar 2D behavior for a quasi-2D gas with $E_F/h\nu_z \simeq 1$, the measured spectra are in strong disagreement with BCS mean-field theory [22], as are the measured thermodynamic properties [21,28–32], which require a beyond mean-field treatment. However, there has been no experimental study of the thermodynamic properties in the nearly 2D regime.

In this Rapid Communication, we study a two-component ^{6}Li Fermi gas in a trap geometry that is smoothly tunable

from 2D to quasi-2D, enabling measurements of both radio-frequency spectra and radial cloud profiles under identical conditions for each regime. For the quasi-2D gas, we find that the spectra are inconsistent with 2D-BCS theory. For the 2D gas, we find that the spectra can be fit by 2D-BCS mean-field theory, consistent with previous work [24,25]. In contrast to the spectra, we find that the radii for 2D clouds are much smaller than those predicted by 2D-BCS mean-field theory, which yields ideal gas density profiles [12]. Our results show that there is no transition between 2D and quasi-2D systems and that beyond mean-field descriptions are required in both cases.

Our experiments, Fig. 1, employ two 1064-nm beams, intersecting at an angle of $91.0°$, creating an array of pancake-shaped optical traps separated by 0.746 μm, which tightly confine atoms along the z axis. Superposed on this periodic array is a focused CO_2 laser beam that provides radial confinement, which controls $\omega_\perp$, the radial harmonic oscillator frequency of a noninteracting atom in the trap. The interaction strength of a balanced (50:50) mixture of atoms in the two lowest hyperfine components (denoted 1 and 2) of ^{6}Li is tuned using the broad Feshbach resonance at 832.2 G [39,40]. By varying the CO_2 laser intensity, we smoothly change $\omega_\perp$ from $2\pi \times 0.36$ kHz to $2\pi \times 2.15$ kHz, which determines the ideal 2D gas radial Fermi energy, $E_F = \hbar\omega_\perp\sqrt{N}$, where $N \simeq 2000$ is the total number of atoms in one site. The interaction strength is characterized by the parameter E_F/E_{b12}, where E_{b12} is the binding energy of a 1–2 dimer in the pancake trap [22]. We choose the dimensionality of each pancake-shaped site by tuning the ratio of E_F to the harmonic oscillator energy level spacing $h\nu_z \equiv 2\sqrt{s}\,E_R$ in the tightly confined z direction, with recoil energy $E_R = h \times 14.9$ kHz and $s\,E_R$ the lattice depth. Using the Kapitza-Dirac effect, we find $s = 15$ and $h\nu_z = h \times 116$ kHz. The cloud is 2D for $E_F/h\nu_z << 1$ and quasi-2D for $E_F/h\nu_z \simeq 1$.

To probe the pairing energy, we use radio-frequency excitation of the transition from the atomic hyperfine state 2 to a higher lying, initially empty hyperfine state 3. We record the number of atoms remaining in state 2 as a function of the excitation frequency relative to the bare atom hyperfine transition frequency, ν_{32}^0 i.e., $\Delta\nu_{rf} \equiv \nu_{rf} - \nu_{32}^0$. We measure ν_{32}^0 using a high-temperature, low-density 1–2 mixture, which agrees with measurements for a noninteracting
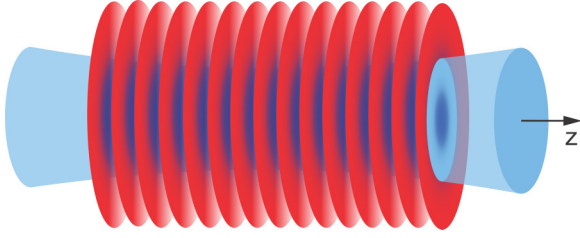
---

*Corresponding author: jethoma7@ncsu.edu

FIG. 1. The radial confinement of a focused CO_2 laser beam (blue) controls the dimensionality of pancake-shaped clouds (red) in a standing-wave optical lattice. The dimensionality of each cloud is determined by the ratio of the radial Fermi energy E_F to the energy level spacing $h\nu_z$ in the tightly confined z direction of each pancake site. Increasing the CO_2 laser intensity tunes the cloud from two-dimensional, where $E_F/h\nu_z \ll 1$, to quasi-2D, where $E_F/h\nu_z \simeq 1$.

cloud containing atoms only in state 2. We then observe the rf spectra in low-temperature mixtures, which exhibit a shifted pairing peak, as shown in Fig. 2 for $B = 1005$ G and in Fig. 3 for $B = 834$ G.

We consider first the measurements in the 2D regime, the upper spectra in Figs. 2 and 3. In our experiments, where $E_F \geqslant E_{b12}$, we expect many-body physics to be important, as the interparticle spacing is then comparable to or smaller than the dimer size. For the 2D regime, we can try to apply 2D-BCS theory for a true 2D system [12]. In this case, the 2D-BCS prediction for a $2 \rightarrow 3$ transition with a noninteracting final state ($E_{b13} \ll E_{b12}$) is $h\Delta\nu_{\rm rf} = E_{b12}$, precisely the dimer pairing energy, as noted previously [22,25]. However, in our experiments E_{b13} is not negligible, so we determine the 2D spectrum including the $\ln(E_{b13}/E_{b12})$ dependence arising from final-state interactions [22,41]. We determine the dimer binding energies in the finite-depth optical lattice using the method of Ref. [42]. The calculated 2D spectra are convolved with a Lorentzian of width w (FWHM). We believe that the linewidth w arises from the short lifetime of the excited state 3 in the 1–2 mixture, as we were not limited by spectroscopic resolution with our pulse duration of 30 ms. For the 2D data, we measure $w = 1.3$ kHz at 1005 G and $w = 4.3$ kHz at 834 G, using the observable atomic $2 \rightarrow 3$ resonance. For the quasi-2D data, the corresponding widths of 4 and 12 kHz are found by fitting, because we could not measure the spectrum of the atomic resonance contribution. For the upper (2D) spectra in Figs. 2 and 3, where $E_F/h\nu_z = 0.16$ and 0.13, respectively, we find that dimer spectra, as predicted by 2D-BCS theory, are in very good agreement with the data, as shown by the calculated red curves.

Now we examine the measurements in the quasi-2D regime, shown as the lower spectra in Figs. 2 and 3, where $E_F/h\nu_z \geqslant 0.67$. Here, we find that 2D-BCS theory does not fit the data. Recently, zero-temperature 2D-BCS theory has been extended to include higher axial states [19], which one expects would contribute in the quasi-2D regime. The predictions show that in the quasi-2D regime, the pairing resonances should be significantly shifted upward in frequency as observed, but quantitative agreement is not obtained [43].

We also consider a 2D-Fermi-polaron model, where spin-down atoms act as impurities dressed by particle-hole clouds in
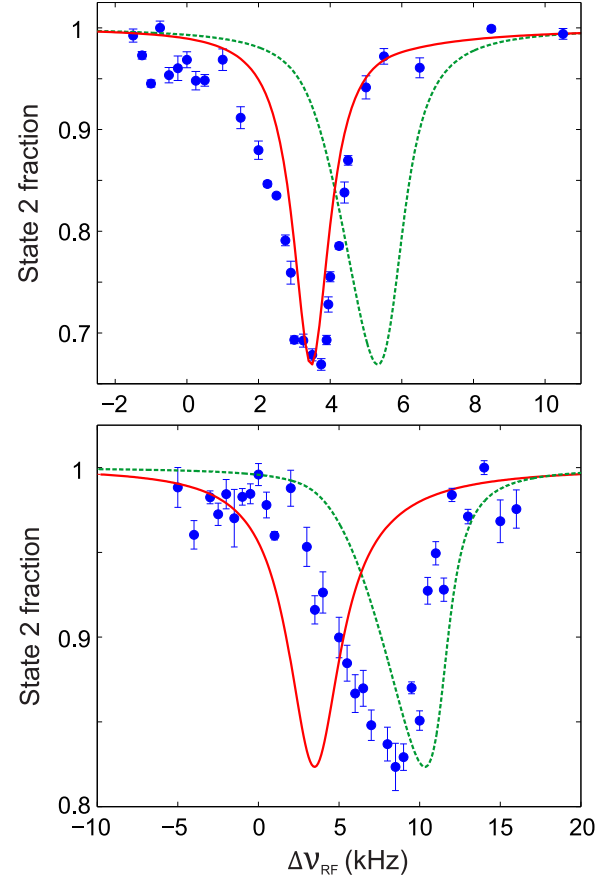

FIG. 2. Radio-frequency spectra at $B = 1005$ G with $\nu_z = 116$ kHz. Top: 2D regime with $E_F/h\nu_z = 0.16$, $E_{b12}/h\nu_z = 0.044$, $E_F/E_{b12} = 3.57$, and $E_{b13}/h\nu_z = 0.016$. Bottom: Quasi-2D regime with $E_F/h\nu_z = 0.75$, $E_{b12}/h\nu_z = 0.044$, $E_F/E_{b12} = 17.1$, and $E_{b13}/h\nu_z = 0.016$. The fraction of atoms remaining in hyperfine state 2 is measured as a function of radio frequency relative to the bare atom $2 \rightarrow 3$ resonance frequency. The solid-red (dashed-green) curves denote the dimer (polaron) prediction with no free parameters (top) and fitted width $w = 4$ kHz (bottom).

a sea of spin-up atoms. We extend this picture by assuming that the polarons are fermionic and weakly interacting, so that the model is applicable even for a 50-50 mixture of both spin states. This heuristic model predicts several features of our previous data in the quasi-2D regime [22,29] and is consistent with more detailed treatments based on the Bethe-Goldstone equation [44,45], which describes two-body interactions in a many-body system. In the spectra, the model predicts a resonance for $h\Delta\nu_{\rm rf} = E_{p13} - E_{p12}$, where the energy of each state is given by

$$E_p = y(q)\epsilon_F. \qquad (1)$$

Here, $\epsilon_F = \pi \hbar^2 n/m$ is the local Fermi energy, m is the atom mass, and n is the total density for the 50:50 mixture. An approximate form for the dimensionless factor $y(q)$ is [44,45]

$$y(q) = \frac{-2}{\ln(1 + 2q)}, \qquad (2)$$

where $q = \epsilon_F/E_b$. This analytic result interpolates between the molecular regime (neglecting the molecular mean field)
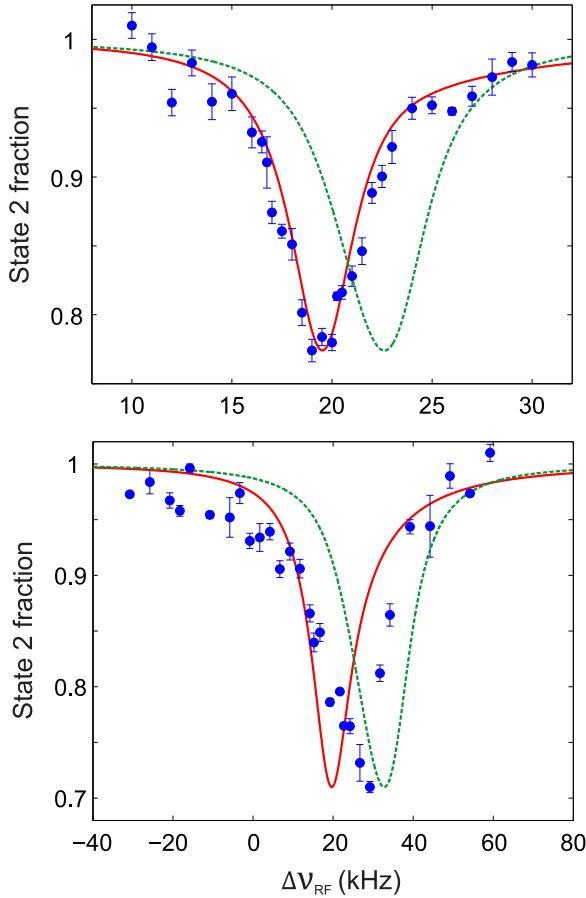
FIG. 3. Radio-frequency spectra at $B = 834$ G with $\nu_z = 116$ kHz. Top: 2D regime with $E_F/h\nu_z = 0.125$, $E_{b12}/h\nu_z = 0.20$, $E_F/E_{b12} = 0.62$, and $E_{b13}/h\nu_z = 0.032$. Bottom: Quasi-2D regime with $E_F/h\nu_z = 0.67$, $E_{b12}/h\nu_z = 0.20$, $E_F/E_{b12} = 3.32$, and $E_{b13}/h\nu_z = 0.032$. The fraction of atoms remaining in hyperfine state 2 is measured as a function of radio-frequency relative to the bare atom $2 \rightarrow 3$ resonance frequency. The solid-red (dashed-green) curves denote the dimer (polaron) prediction with no free parameters (top) and fitted width $w = 12$ kHz (bottom).

at magnetic fields well below the Feshbach resonance and agrees with the Fermi polaron approximation [22] and recent quantum Monte Carlo predictions [46] for $\epsilon_F/E_b > 3$. The dashed-green curves in the spectra of Figs. 2 and 3 show the predictions using Eq. (2), with

$$I(\Delta\nu) \propto \int \frac{2\pi\rho \, d\rho \, n(\rho)}{1 + (2/w)^2[\Delta\nu - (E_{p13} - E_{p12})/h]^2}, \quad (3)$$

where the 2D-density $n(\rho)$ is determined from fits to the measured column density profiles. As the density decreases, the local Fermi energy decreases from its maximum value, producing a downward-sweeping broad spectrum, consistent with the data. We see that the 2D-polaron spectrum based on Eq. (2) predicts resonances in reasonable agreement with the quasi-2D data.

In previous studies of quasi-2D spin-imbalanced and spin-balanced clouds [29], we measured both the cloud radii and the pressure for $E_F/h\nu_z = 1.5$. There, we found that the 2D-polaron model gives a reasonable fit for the measured radii
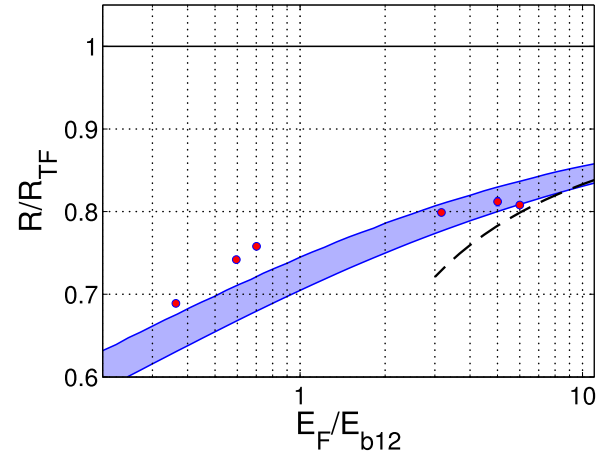

FIG. 4. Cloud radii versus E_F/E_b, where E_F is the radial Fermi energy for an ideal gas, $R_{\rm TF}$ is the Thomas-Fermi radius, and E_{b12} is the 2D dimer binding energy of a 1–2 atom pair. The blue band shows 2D-polaron model prediction at $T = 0$ (lower side) and $T/T_F = 0.2$ (upper side). The solid line at $R/R_{\rm TF} = 1$ is the 2D-BCS prediction. The dashed curve is the Fermi liquid limit, $R/R_{\rm TF} \simeq 1 - 0.5/\ln(2E_F/E_{b12})$. Note that the statistical error bars are comparable to the point size.

and pressure, while 2D-BCS theory for a balanced gas predicts an ideal gas pressure and ideal gas cloud profiles [12,29], in strong disagreement with the measurements. Recently, Fischer and Parish [6] extended finite-temperature 2D-BCS theory to include higher axial states, which are expected to contribute to the thermodynamics in the quasi-2D regime. In this case, the predicted pressure decreases below the ideal gas pressure with increasing $E_F/h\nu_z$, but it is well above the 2D-polaron prediction [29], which agrees with measurements in the quasi-2D regime [21,29].

Our measured spectra for the 2D regime appear to agree with 2D-BCS mean-field theory, which predicts dimer spectra, consistent with the 2D spectra obtained in Refs. [24,25]. To examine the 2D-BCS predictions further, we use an *in situ* phase-contrast method to image the dense clouds in the 2D regime with $E_F/h\nu_z \leqslant 0.18$. From the atom number and peak column density [29], we obtain the cloud radii shown in Fig. 4.

Over the measured range of E_F/E_b, we see that the cloud radii are well below the ideal gas limit $R/R_{\rm TF} = 1$, where $R_{\rm TF} = \sqrt{2E_F/m\omega_\perp^2}$ is the Thomas-Fermi radius. In contrast, 2D-BCS theory for a true 2D system predicts ideal gas Thomas-Fermi profiles [12,29], $R/R_{\rm TF} = 1$, in strong disagreement with the data.

Now we consider the 2D-polaron model prediction, shown as the the lower side of the blue band in Fig. 4. The cloud radii are determined from the local chemical potential $\mu = \partial f/\partial n$, which is determined from the approximate free energy density for the balanced gas [29,45],

$$f = \frac{n}{2} \epsilon_F [1 + y(q)]. \quad (4)$$

For the spin-balanced 1–2 mixture, using Eq. (2), we obtain the cloud radii in units of the ideal gas Thomas-Fermi

radius [29],

$$\frac{R}{R_{\text{TF}}} = \sqrt{\tilde{\mu}(0) + \frac{E_{b12}}{2E_F}}, \qquad (5)$$

where $\tilde{\mu}(0)$ is the chemical potential at the center of the cloud in units of E_F, which is self-consistently determined [47]. For large values of $\eta \equiv \ln(\sqrt{2E_F/E_{b12}}) \simeq \ln(k_F a_{2D})$, expansion of Eq. (5) to lowest order in $1/\eta$ leads to $R/R_{\text{TF}} \simeq 1 - 1/(4\eta)$, the density profile of a Fermi liquid [48] in a harmonic trap. Here, k_F is the Fermi momentum and a_{2D} is the 2D scattering length. We plot the Fermi liquid result as the dashed curve in Fig. 4.

For these experiments, we are not able to cool the cloud as efficiently as in our previous studies in a CO_2 laser lattice, where we obtained $T/T_F < 0.2$. We estimate the effect of finite temperature by using ideal gas temperature scaling for the zero-temperature radii. For $T/T_F = 0.2$, we obtain the upper side of the blue band in Fig. 4.

In conclusion, we have measured the pairing energy and cloud radii for nearly 2D and quasi-2D Fermi gases. Our results clearly confirm theoretical predictions that a beyond mean-field description is required throughout the 2D to quasi-2D crossover.

[1] C. C. Tsuei and J. R. Kirtley, Rev. Mod. Phys. **72**, 969 (2000).

[2] J. Singleton and C. Mielke, Contemp. Phys. **43**, 63 (2002).

[3] D. L. Smith and C. Mailhiot, Rev. Mod. Phys. **62**, 173 (1990).

[4] M. R. Norman, Science **332**, 196 (2011).

[5] M. A. Baranov, D. V. Efremov, and M. Yu. Kagan, Physica C: Superconductivity **218**, 75 (1993).

[6] A. M. Fischer and M. M. Parish, Phys. Rev. B **90**, 214503 (2014).

[7] M. Randeria, J.-M. Duan, and L.-Y. Shieh, Phys. Rev. Lett. **62**, 981 (1989).

[8] H. Caldas, A. L. Mota, R. L. S. Farias, and L. A. Souza, J. Stat. Mech. (2012) P10019.

[9] S. Yin, J.-P. Martikainen, and P. Törmä, Phys. Rev. B **89**, 014507 (2014).

[10] J.-P. Martikainen and P. Törmä, Phys. Rev. Lett. **95**, 170407 (2005).

[11] S. S. Botelho and C. A. R. Sá de Melo, Phys. Rev. Lett. **96**, 040404 (2006).

[12] L. He and P. Zhuang, Phys. Rev. A **78**, 033613 (2008).

[13] W. Zhang, G.-D. Lin, and L.-M. Duan, Phys. Rev. A **78**, 043617 (2008).

[14] J. Tempere, S. N. Klimin, and J. T. Devreese, Phys. Rev. A **79**, 053637 (2009).

[15] G. Bertaina and S. Giorgini, Phys. Rev. Lett. **106**, 110403 (2011).

[16] M. Bauer, M. M. Parish, and T. Enss, Phys. Rev. Lett. **112**, 135302 (2014).

[17] D. E. Sheehy, Phys. Rev. A **92**, 053631 (2015).

[18] L. He, H. Lü, G. Cao, H. Hu, and X.-J. Liu, Phys. Rev. A **92**, 023620 (2015).

[19] A. M. Fischer and M. M. Parish, Phys. Rev. A **88**, 023612 (2013).

[20] K. Martiyanov, V. Makhalov, and A. Turlapov, Phys. Rev. Lett. **105**, 030404 (2010).

[21] V. Makhalov, K. Martiyanov, and A. Turlapov, Phys. Rev. Lett. **112**, 045301 (2014).

[22] Y. Zhang, W. Ong, I. Arakelyan, and J. E. Thomas, Phys. Rev. Lett. **108**, 235302 (2012).

[23] M. Feld, B. Frohlich, E. Vogt, M. Koschorreck, and M. Kohl, Nature **480**, 75 (2011).

[24] B. Fröhlich, M. Feld, E. Vogt, M. Koschorreck, W. Zwerger, and M. Köhl, Phys. Rev. Lett. **106**, 105301 (2011).

[25] A. T. Sommer, L. W. Cheuk, M. J. H. Ku, W. S. Bakr, and M. W. Zwierlein, Phys. Rev. Lett. **108**, 045302 (2012).

[26] M. Koschorreck, D. Pertot, E. Vogt, B. Frohlich, M. Feld, and M. Kohl, Nature **485**, 619 (2012).

[27] A. A. Orel, P. Dyke, M. Delehaye, C. J. Vale, and H. Hu, New J. Phys. **13**, 113032 (2011).

[28] M. G. Ries, A. N. Wenz, G. Zürn, L. Bayha, I. Boettcher, D. Kedar, P. A. Murthy, M. Neidig, T. Lompe, and S. Jochim, Phys. Rev. Lett. **114**, 230401 (2015).

[29] W. Ong, C. Cheng, I. Arakelyan, and J. E. Thomas, Phys. Rev. Lett. **114**, 110403 (2015).

[30] I. Boettcher, L. Bayha, D. Kedar, P. A. Murthy, M. Neidig, M. G. Ries, A. N. Wenz, G. Zürn, S. Jochim, and T. Enss, Phys. Rev. Lett. **116**, 045303 (2016).

[31] K. Fenech, P. Dyke, T. Peppler, M. G. Lingham, S. Hoinka, H. Hu, and C. J. Vale, Phys. Rev. Lett. **116**, 045302 (2016).

[32] P. A. Murthy, I. Boettcher, L. Bayha, M. Holzmann, D. Kedar, M. Neidig, M. G. Ries, A. N. Wenz, G. Zürn, and S. Jochim, Phys. Rev. Lett. **115**, 010401 (2015).

[33] D. S. Petrov and G. V. Shlyapnikov, Phys. Rev. A **64**, 012706 (2001).

[34] M. Randeria and E. Taylor, Annu. Rev. Condens. Matt. Phys. **5**, 209 (2014).

[35] E. R. Anderson and J. E. Drut, Phys. Rev. Lett. **115**, 115301 (2015).

[36] H. Shi, S. Chiesa, and S. Zhang, Phys. Rev. A **92**, 033603 (2015).

[37] A. Galea, H. Dawkins, S. Gandolfi, and A. Gezerlis, Phys. Rev. A **93**, 023602 (2016).

[38] B. C. Mulkerin, K. Fenech, P. Dyke, C. J. Vale, X.-J. Liu, and H. Hu, Phys. Rev. A **92**, 063636 (2015).

[39] M. Bartenstein, A. Altmeyer, S. Riedl, R. Geursen, S. Jochim, C. Chin, J. H. Denschlag, R. Grimm, A. Simoni, E. Tiesinga, C. J. Williams, and P. S. Julienne, Phys. Rev. Lett. **94**, 103201 (2005).

[40] G. Zürn, T. Lompe, A. N. Wenz, S. Jochim, P. S. Julienne, and J. M. Hutson, Phys. Rev. Lett. **110**, 135301 (2013).

[41] C. Langmack, M. Barth, W. Zwerger, and E. Braaten, Phys. Rev. Lett. **108**, 060402 (2012).

[42] G. Orso, L. P. Pitaevskii, S. Stringari, and M. Wouters, Phys. Rev. Lett. **95**, 060402 (2005).

[43] Meera Parish (private communication).

[44] M. Klawunn and A. Recati, Phys. Rev. A **84**, 033607 (2011).

[45] M. Klawunn, Phys. Lett. A **380**, 2650 (2016).

[46] S. Bour, D. Lee, H.-W. Hammer, and Ulf-G. Meißner, Phys. Rev. Lett. **115**, 185301 (2015).

[47] Here, $\tilde{\mu}(0) = \tilde{n}(0)\{1 + y_m[q_0\tilde{n}(0)] + y'_m[q_0\tilde{n}(0)]/2\}$, where $y'_m(q) \equiv q\, y_m^2(q)/(1 + 2q)$ and $q_0 = E_F/E_b$. We determine the scaled total density $\tilde{n}(0)$ self-consistently from $\tilde{n}(0) = 1/\sqrt{1 + y_m[q_0\tilde{n}(0)] + y'_m[q_0\tilde{n}(0)]}$. For a detailed explanation, see the Supplementary Material of Ref. [29].

[48] P. Bloom, Phys. Rev. B **12**, 125 (1975).